Materials Science in Semiconductor Processing 80 (2018) 174–178

Contents lists available at ScienceDirect

Materials Science in Semiconductor Processing

journal homepage: www.elsevier.com/locate/mssp

Distinctive electroluminescence characteristics behind efficient mesoscopic perovskite solar cell

Minhuan Wang[a], Jiming Bian[a,*], Yulin Feng[a], Qingshun Dong[b], Bingye Zhang[a], Hongzhu Liu[a], Yantao Shi[b,*]

[a] Key Laboratory of Materials Modification by Laser, Ion and Electron Beams (Ministry of Education), School of Physics, Dalian University of Technology, Dalian 116024, China

[b] State Key Laboratory of Fine Chemicals, School of Chemistry, Dalian University of Technology, Dalian 116024, China

ARTICLE INFO

Keywords:
Perovskite solar cells
Perovskite light emitting diode
Time-resolved electroluminescence
SnO_2 electron transport layer

ABSTRACT

Metal halide perovskites are emerging as exceptional class of materials due to its unprecedented collective advantages for optoelectronic applications. Here, the efficient mesoscopic perovskite solar cells (M-PSCs) with the architecture of FTO-SnO_2/m-TiO_2 + $MAPbI_3$/Spiro-OMeTAD/Ag were synthesized, where the discontinuous SnO_2 derived blended-interfacial-layer worked as electron transport layer (ETL). A moderate power conversion efficiencies (PCEs) of 17.42% was achieved. Notably, a 10 s level ultra-long rise time in time-resolved electroluminescence (EL) characteristics was observed from the same device as the $MAPbI_3$ perovskite layer served as light emitter. Such performance was attributed to the reasonable device design based on the dynamics favorable electron transport layer. This achievement would be beneficial for further understanding the working mechanism of perovskite-based optical-to-electrical and electrical-to-optical conversion devices.

1. Introduction

Organic-inorganic halide perovskite (OIHP) have drawn global interest due to its significant potential for optoelectronic applications. The rise in power conversion efficiencies (PCEs) of perovskite solar cells (PSCs) has shown unprecedented speed and certified values exceed 22% has been achieved recently [1–7]. In addition, the OIHP should also be an ideal light emitter according to the detailed balance in the Shockley-Queisser formulation [8]. Following this idea, perovskite light-emitting diodes (Pe-LEDs) with strong electroluminescence (EL) intensity and tunable emission spectra have also been achieved, which maybe suitable for next-generation high-definition displays and healthy lighting systems [9,10]. The great success of OIHP for both PSCs and Pe-LEDs was mainly ascribed to their unprecedented outstanding properties, including a narrow bandwidth, precise and facile tunable luminance over the entire visible spectrum, and high photoluminescence quantum yield (PLQY). [11]. However, the working mechanism of perovskite-based energy conversion devices, particularly the charge carriers transport and recombination mechanism, have not been well understood by far, which would be prerequisite and foundation for further boosting the performance and reliable perovskite devices (PSCs or/and Pe-LEDs). Moreover, although it has been reported that PSCs that can also be operated as Pe-LED devices, rather inferior performance were usually demonstrated for Pe-LEDs from PSCs device with the same architecture due to the substantial divergence in material requirement for photovoltaic and light emission [10,12,13].

To further improve the performance and long-term durability of perovskite based optoelectronic devices, more elaborate construction of each function layer is necessary [14–17]. In our recent studies, mesoscopic perovskite solar cell (M-PSCs) with discontinuous SnO_2 derived blended-interfacial-layer as electron transport layer (ETL) were synthesized, and a much improved photovoltaic performance was achieved compared with the counterpart with traditional TiO_2 ETL design [18,19]. Nevertheless, there has been no report on the time resolved EL characteristics behind the efficient M-PSCs, which was considered to be essential for further exploiting the advantageous with this novel ETL strategy.

In this paper, the M-PSCs were synthesized with the structure of FTO-SnO_2/m-TiO_2 + $CH_3NH_3PbI_3$ (henceforth $MAPbI_3$)/Spiro-OMeTAD/Ag. A moderate PCEs of 17.42% was achieved from the M-PSCs. Notably, a 10 s scale ultra-long rise time (T_r) was observed in the time resolved EL characteristics from the device as the $MAPbI_3$ perovskite photoactive layer served as light emitting layer, which is far beyond the T_r for traditional organic LEDs or GaN based inorganic LEDs [20–23]. The possible mechanism responsible for the delayed EL was proposed. Our research will provide more insight into the working

* Corresponding authors.
E-mail addresses: jmbian@dlut.edu.cn (J. Bian), shiyantao@dlut.edu.cn (Y. Shi).

https://doi.org/10.1016/j.mssp.2018.01.028
Received 9 January 2018; Accepted 27 January 2018

mechanism of perovskite-based energy conversion devices like Pe-LEDs and PSCs.

2. Experimental details

2.1. Device fabrication

The detailed device fabrication process for M-PSCs with the structure of FTO-SnO_2/m-TiO_2 + $MAPbI_3$/Spiro-OMeTAD/Ag have been reported in our recent report [19]. Briefly, SnO_2 sol was first spread onto patterned FTO glass substrate followed by sintering at 450 °C for 1 h. Next, mesoporous TiO_2 scaffold layer was deposited by spin coating followed by the deposition of $MAPbI_3$ perovskite layer with the well-established two-step process in our lab [18]. Then, the Spiro-OMeTAD layer served as hole transport layer (HTL) was deposited on the $MAPbI_3$ perovskite layer. Finally, silver cathode with a thickness of ~ 60 nm was thermally deposited atop the Spiro-OMeTAD layer. The device working area was fixed at 0.12 cm^2 as defined by the overlap of the FTO substrate and the Ag cathode. All the devices process were carried out in a glove box to avoid exposing to ambient atmosphere.

2.2. Characterizations

The microstructures of the device were observed by a field emission scanning electron microscope (FE-SEM; S4800). The composition and elemental distribution of the heterostructure were studied by X-ray energy dispersive spectroscopy (EDS) attached to the SEM. During EL spectra measurement, the device was electrically driven with the positive voltage connected with the Ag electrode. The EL properties were recorded by the FLS920 fluorescence spectrometer at continuous current injection, while the steady-state and time-resolved PL measurements were performed by the same spectrometer using 310 nm line of a 450 W steady state xenon lamp (Xe900) as excitation source. The *J-V* characteristics were measured using Keithley 2450 source meter at room temperature, and the photovoltaic response of the M-PSCs was obtained by recording the *J-V* curves under the irradiation of Solar simulator AM 1.5 (100 mW cm^{-2}, Solar3A, Newport). The physical photos of the perovskite device were photographed by infrared camera DFC-F717.

3. Results and discussion

Fig. 1a shows the across-section SEM image of the multilayer perovskite device. As expected, the FTO-SnO_2/m-TiO_2 + $MAPbI_3$/Spiro-OMeTAD/Ag heterostructure with well-defined interface was observed, and each layers were clearly marked with the observed thickness. The $MAPbI_3$ film was infiltrated into the mesoporous TiO_2 (m-TiO_2) scaffolds layer to form the full-coverage and pinhole-free perovskite active layer, on top of which the dense Spiro-OMeTAD layer and Ag electrode were uniformly deposited. In addition, the elemental spatial distribution across the structure identified by EDS analysis (Fig. 1b), was in reasonable agreement with the cross-section SEM image, demonstrating that the abrupt heterostructure with well-defined interfaces and composition distribution was achieved in our multilayer structure. In this configuration, the discontinuous SnO_2 nanocrystallites were concentrated at the low-lying locations of FTO glass, which have been demonstrated to be more kinetically favorable for electron transfer in our recent report [19].

Fig. 2a shows the *J-V* curve of the perovskite device under the irradiation of Solar simulator AM 1.5, a moderate PCEs output of 17.42% was obtained from the M-PSCs device, and the detailed photovoltaic parameters have been reported in our previous report [19]. Fig. 2b is the *J-V* characteristics of the M-PSCs device measured in dark ambient. The distinct diode like rectifying behavior with a forward turn-on voltage of ~ 0.8 V and extremely low reverse current was observed from the asymmetric *J-V* curve. The rather lower turn-on voltage may be attributed to the outstanding electrical properties of the novel FTO-SnO_2 ETL layer which provided a better band alignment for interfacial electron transfer. So the same device can work as M-PSCs or Pe-LEDs depending on the $MAPbI_3$ perovskite layer acted as light harvest or light emitter, and the corresponding schematic diagrams were shown in the inset of Fig. 2a and b, respectively. The good performance of the $MAPbI_3$-based devices for optical-to-electrical and electrical-to-optical energy conversion can be attributed to the high crystalline quality of two-step processed $MAPbI_3$ layer, as well as the reasonable device design based on balanced carrier injection and confinement configuration. As illustrated by the energy band diagram for the multilayer device in Fig. 2c, where the band gap (Eg) and electron affinity (χ) values for each constituent materials were set according to literatures [18–20]. The special position of energy level in the structure, would be especially favorable for the confinement of electrons and holes in the $MAPbI_3$ active layer under forward injection conditions, thus greatly increase the radiative recombination possibility of electron-hole pairs in the Pe-LEDs.

To further investigate the origin and mechanism of the EL emission behind the m-PSCs, Fig. 3a shows the comparison of EL (driving at 1.5 V) and PL (λ_{exc} = 310 nm) spectra from the $MAPbI_3$ active layer deposited directly on FTO-SnO_2 substrate by the same process, where the intensities has been normalized to clearly demonstrate the shift of peak position and spectral shape. A sharp near-infrared emission with the dominant peak centered at 775 nm and almost identical FWHM of 36 nm was detected from both EL and PL spectra, which was in excellent agreement with the optical bandgap of $MAPbI_3$ achieved from optical transmittance measurement [24], also well consistent with the bandgap value of $MAPbI_3$ single crystal [25], suggesting nearly intrinsic band edge emission feature. The perfectly coincidence of the EL and PL spectra provide convincing evidence that the radiative recombination occurred in the $MAPbI_3$ active layer as carriers injected under forward

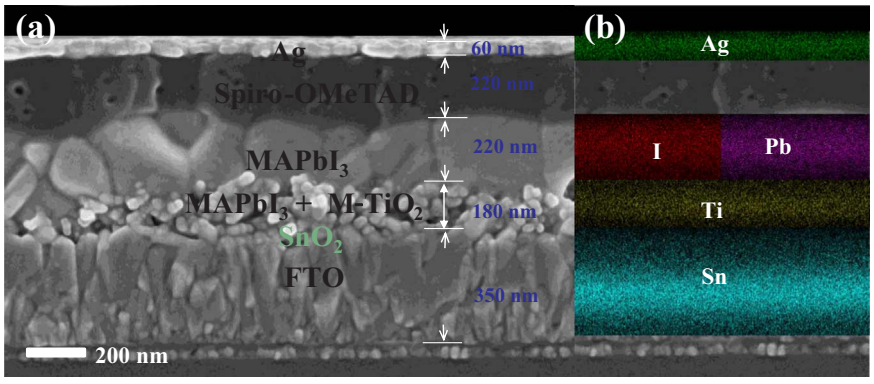

Fig. 1. (a) Cross-section SEM image of the completed FTO-SnO_2/m-TiO_2 + $MAPbI_3$ /Spiro-OMeTAD/Ag multilayer device and the corresponding elemental mapping images by EDS shown in (b).